Published in Optics Express 14, issue 11, 4687-4694, 2006
which should be used for any reference to this work

On the chromatic aberration of microlenses

Patrick Ruffieux, Toralf Scharf, and Hans Peter Herzig

University of Neuchâtel, Institute of Microtechnology,
Patrick.Ruffieux@unine.ch; Toralf.Scharf@unine.ch; HansPeter.Herzig@unine.ch

Reinhard Völkel, and Kenneth J. Weible

SUSS MicroOptics SA
voelkel@suss.ch; weible@suss.ch

Abstract: The optical properties of plano-convex refractive microlenses with low Fresnel Number (typically FN < 10) are investigated. It turns out that diffraction effects at the lens aperture limit the range of the effective focal length. The upper limit of the focal length is determined by the diffraction pattern of a pinhole with equal diameter. In addition achromatic microlenses can be realized because refraction and diffraction have opposing effects on the focal length. Gaussian beam propagation method has been used for simulation. The presented results are of relevance for applications, where microlenses with small apertures and long focal lengths are used, for example, Shack Hartmann wavefront sensors or confocal microscopes.

References

1. D. Malacara, and Z. Malacara, *Handbook of lens design*, (Dekker, New York, 1994).
2. Y. Li, and E. Wolf, "Focal shifts in diffracted converging spherical waves," Opt. Commun. **39,** 211 (1981).
3. Y. Li, and H. Platzer, "An experimental investigation of diffraction patterns in low Fresnel-number focusing systems," Optica Acta **30,** 1621 (1983).
4. W. Wang, A. T. Friberg, E. Wolf, "Structure of focused fields in systems with large Fresnel numbers," J. Opt. Soc. Am. A. **12,** 1947 (1995).
5. J. Arnaud, "Representation of Gaussian beams by complex rays," Appl. Opt. **24**, (1985).
6. U. Vokinger, R. Dändliker, P. Blattner, and H. P. Herzig, "Unconventional treatment of focal shift," Opt. Commun. **157,** 218-224 (1998).
7. J. W. Goodman, *Introduction to Fourier Optics*, 2nd ed., (MacGraw-Hill, New York, 1968), Chap. 4, pp. 63-69.

1. Introduction

The refractive index of any transparent material is function of the wavelength. Therefore, a lens made in one single material shows different positions of focus at each wavelength. The difference in position of these focal points is known as the longitudinal primary chromatic aberration [1]. To correct this aberration, achromatic lenses are usually manufactured using two lenses of different material having different Abbe numbers combined to form a doublet or even triplet [1]. This method uses the different dispersion curves of the materials to obtain, at two well separated wavelengths, the same focal length with small variations for the other wavelengths in between. By their small dimensions microlenses can have low Fresnel number and then exhibit strong diffractive effects on the position and the shape of their focal point as it has been extensively studied in literature (focal shift [2] [3] [4]). We show here that for such lenses a range for the radius of curvature (ROC) can be found where microlenses show an achromatic behavior. Firstly we focus our study on the position of the peak irradiance (Z_p) for different microlenses diameters as function of ROC. The focal length is increased by increasing the ROC. However at a certain value for ROC, the focal length cannot be further

increased. The limit is fixed by the position of the peak irradiance of the light diffracted by an aperture equal to the lens diameter. Secondly we study the position of the peak irradiance at different wavelengths. We observe two phenomena influencing Z_p. One is the focal shift due to diffraction and the second is the chromatic aberration due to the material dispersion. Because these two phenomena have opposing influence on Z_p, a choice for the ROC can be found where Z_p is the same at two wavelengths. This property could be used to design achromatic lenses in one single material.

2. Basic considerations

The focal length f_E of a plano-convex refractive lens is derived from the radius of curvature ROC and the refractive index n of the lens material

$$f_E = \frac{ROC}{(n-1)} \cdot \tag{1}$$

The refractive index is a function of the wavelength λ, whereas $n(\lambda_2) < n(\lambda_1)$ for $\lambda_2 > \lambda_1$. The longitudinal primary chromatic aberration, corresponds to a chromatic shift of the focal length, $f_E(\lambda_2) > f_E(\lambda_1)$ for $\lambda_2 > \lambda_1$, [1]. The Fresnel number FN of a lens with a lens diameter Ø = 2ρ is defined by

$$FN = \frac{\rho^2}{\lambda f_E} \cdot \tag{2}$$

For large Fresnel numbers FN >> 1, geometric optics is well suitable to derive the focal length of a microlens. For low Fresnel numbers, the focal length is shifted towards the lens due to the influence of the diffraction at the lens stop. A Gaussian beam decomposition algorithm [5] is used for the comprehensive analysis of the refractive and diffractive properties of the microlenses.

3. Plano-convex refractive microlens

A plane wave with constant intensity profile illuminates a plano-convex refractive microlens as shown in Fig. 1. An aperture blocks the light outside the microlens.

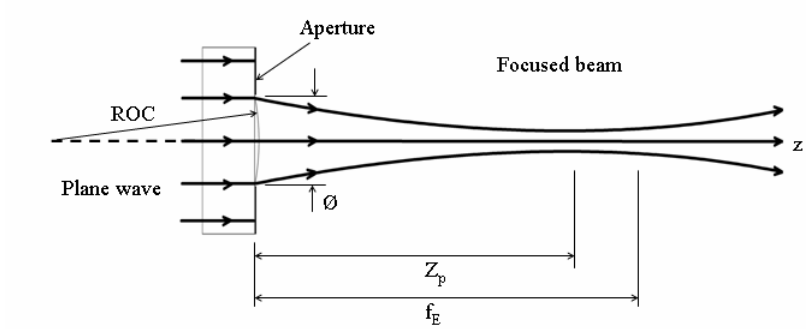

Fig. 1. Model of a plano-convex microlens illuminated by a plane wave.

As an example, a microlens with diameter Ø = 635 µm, ROC = 2.03 mm, made of fused silica with n (633 nm) = 1.456 has been chosen. From paraxial geometric optics, the focal length is f_E = 4.45 mm. The Fresnel number of the lens is FN = 35.7. As shown in Fig. 2, diffraction analysis [5] predicts a position of the peak irradiance Z_p at 4.36 mm. The difference between the position of the peak irradiance Z_p derived from diffraction theory and the focal length f_E obtained from geometrical optics is defined as focal shift δ [6]:

$$\delta = Z_p - f_E \cdot \tag{3}$$

In the example of a microlens with a Fresnel number FN = 35.7. A focal shift of δ = -0.09 mm, corresponding to 2% mismatch is observed. This shows a good agreement between geometrical optics and diffraction theory for microlenses with large Fresnel numbers.

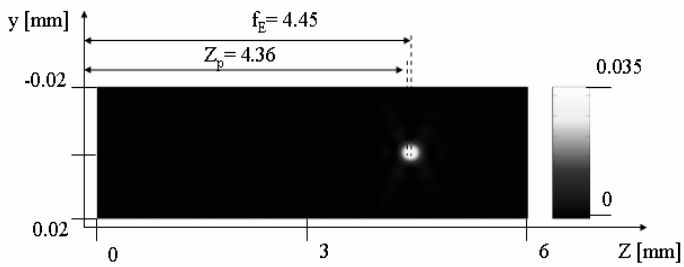

Fig. 2. Intensity (a.u.) distribution behind a microlens of Ø = 635 μm, ROC = 2.03 mm, illuminated by a plane wave at 633 nm. The lens stands in the x,y plan while z corresponds to the propagating axis.

Figure 3 shows the intensity distribution of a microlens with a Fresnel number FN = 6.29. A focal shift of δ = -6.23 mm, corresponding to 11% mismatch is observed.

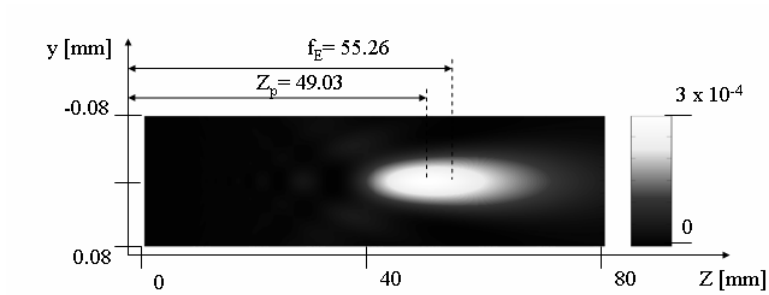

Fig. 3. Intensity (a.u.) distribution behind a microlens of Ø = 635 μm and ROC = 25.2 mm illuminated by a plane wave at 633 nm. The lens stands in the x,y plan while z corresponds to the propagating axis.

Figure 4 shows the intensity distribution of a microlens with a Fresnel number FN = 0.3. A focal shift of δ = -416.86 mm, corresponding to 75% mismatch is observed.

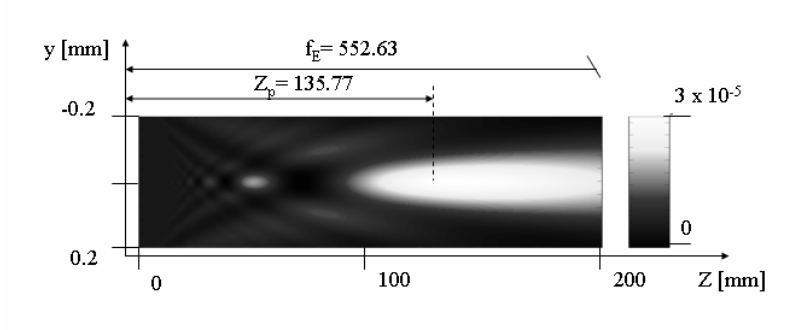

Fig. 4. Intensity (a.u.) distribution behind a microlens of Ø = 635 µm, ROC = 252 mm, illuminated by a plane wave at 633 nm. The lens stands in the x,y plan while z corresponds to the propagating axis.

Figure 5 shows the intensity distribution behind a pinhole with same diameter. A pinhole with no refractive power corresponds to a microlens with ROC = ∞.

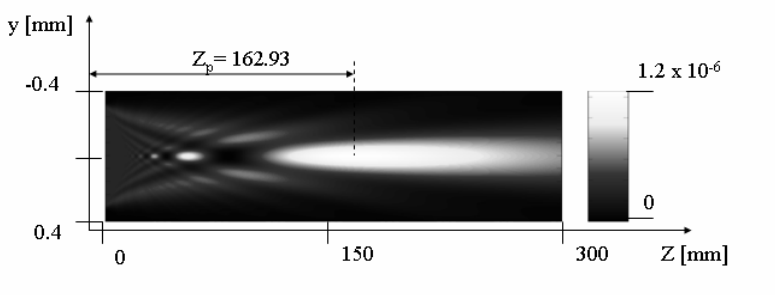

Fig. 5. Intensity (a.u.) distribution behind an aperture of Ø = 635 µm illuminated by a plane wave at 633 nm. The lens stands in the x,y plan while z corresponds to the propagating axis.

The observed peak irradiance position Z_p = 162.93 mm is the maximum obtainable focus spot position for a microlens of Ø = 635 µm diameter.

4. Refractive and diffractive regime

These phenomena are now analyzed for different microlens diameters illuminated by a plane wave at 633 nm.

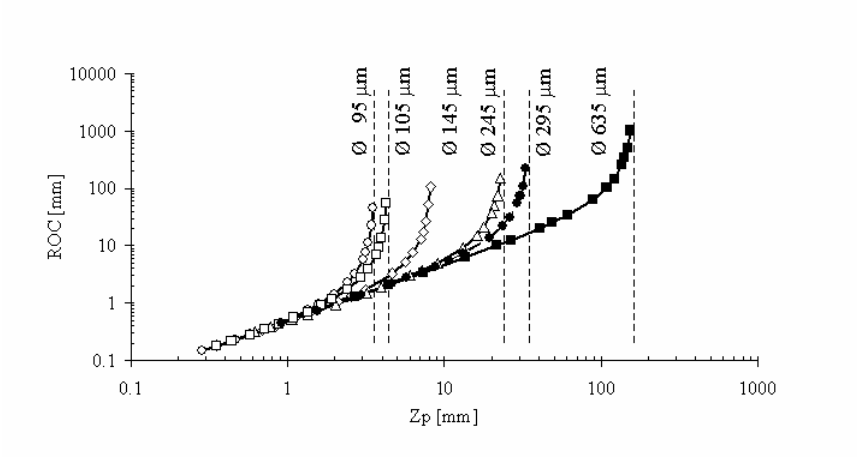

Fig. 6. ROC [mm] versus position of peak irradiance for six diameters of microlenses illuminated by a plane wave at 633nm.

Figure 6 shows Z_p function of ROC for different microlens diameters. For low ROC (typically ROC < 1 mm for Ø = 635 µm microlens) the peak irradiance corresponds to the focal length obtained by Eq. (1). For increasing values of ROC, the peak irradiance converges to a maximum value $Z_{p\,max}$ illustrated by vertical dash lines in Fig. 6. This value corresponds to the peak irradiance position obtained for a pinhole with no optical power, i.e. ROC = ∞. To check the validity of the present approach, the values of $Z_{p\,max}$ obtained by the Gaussian beam decomposition algorithm are now compared to the values derived from the Rayleigh-Sommerfeld integral.

The scalar field U(**r**,z) at the point P is given by [7],

$$U(\mathbf{r},z)=\frac{1}{i\lambda}\int_{\Sigma}A_0(\mathbf{r}_0)\frac{\exp(ikR)}{R}\cos(\theta)dS\,, \tag{4}$$

where Σ is the surface limited by the aperture in $z_0 = 0$. For a plane wave diffracted at the circular aperture and propagating along the optical axis we have $A_0(\mathbf{r}_0)=A_0$ and $R=\sqrt{z^2+\mathbf{r}_0^{\,2}}$ with $r_0=|\mathbf{r_0}|$. Furthermore, for paraxial approximation we assume that $\mathbf{cos}(\theta)\approx 1$. Substituting these relations into Eq. (4) and introducing polar co-ordinates yields to

$$U(\mathbf{r}=0,\mathrm{z}\ )=\frac{A_0}{i\lambda}\int_{\varphi=0}^{2\pi}\int_{r_0=0}^{\rho_0}\frac{\exp\left(ik\sqrt{z^2+r^2{}_0}\right)}{\sqrt{z^2+r^2{}_0}}r_0dr_0d\phi\,, \tag{5}$$

where ρ_0 is the radius of the limiting aperture at $z_0=0$. Integrating Eq. (5) and approximating the square root in the phase by the first two terms of the Taylor series yields to

$$I(\mathbf{r}=0,\mathrm{z})=\left(2A_0\sin\left(\frac{k\rho^2{}_0}{4z}\right)\right)^2, \tag{6}$$

describing the intensity distribution along the optical axis. The maximum intensity is found by setting the derivative of Eq. (6) equal to zero,

$$\frac{dI(\mathbf{r}=0,\mathrm{z})}{dz}=-A_0k\rho_0{}^2\sin\left(\frac{k\rho^2{}_0}{2z}\right)\frac{1}{z^2}=0\,, \tag{7}$$

which implies that $\frac{k\rho_0^2}{2z} = \pi$. The position of peak irradiance of an aperture obtained by the Rayleigh-Sommerfeld integral is

$$Z_p = \frac{\rho_0^2}{\lambda}. \tag{8}$$

The peak irradiance positions Z_p of pinholes with $Ø = 2\rho_0$ diameters obtained from Rayleigh-Sommerfeld, are shown as dashed lines in Fig. 6. The Gaussian beam decomposition algorithm corresponds well to the Rayleigh-Sommerfeld approach.

5. Achromaticity

As described in the previous section microlenses exhibit a refractive regime following the linear law predicted by classical optics and a diffractive regime where the peak irradiance converges to a maximum value. As shown in Fig. 7, both effects are related to the wavelength λ. In the diffractive regime, the peak irradiance Z_p is strongly dominated by the focal shift introduced by diffraction at the aperture and converges to a maximum value proportional to the inverse of the wavelength, see Eq. (8).

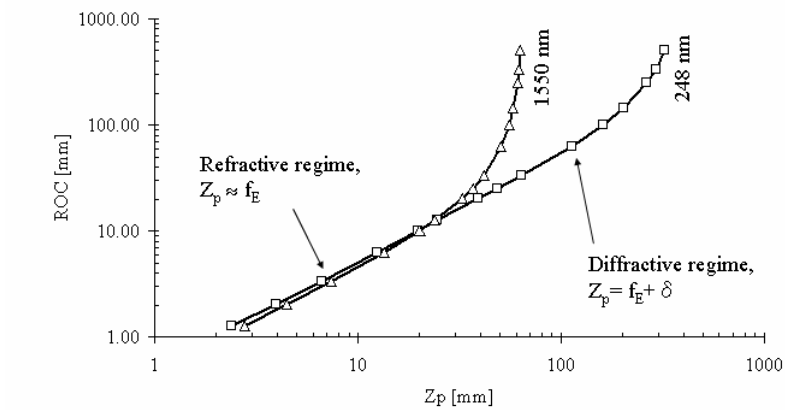

Fig. 7. ROC versus position of peak irradiance Z_p for microlenses of Ø = 635 µm illuminated by a plane wave at two different wavelengths.

In the refractive domain, the peak irradiance Z_p respectively the focal length f_E is inversely proportional to the refractive index n(λ). The dispersion curve of a material approximated by the Cauchy Formula [1] Eq. (9),

$$n = C_0 + \frac{C_1}{\lambda^2} + \frac{C_2}{\lambda^4}, \tag{9}$$

leads to a decreasing refractive index for increasing wavelengths. In the refractive regime, the position of the peak irradiance (Z_p) is equal to the focal length given by Eq. (1).

Figure 8 shows the peak irradiance position function of ROC at different wavelengths λ. The longitudinal primary chromatic aberration δ_λ is the difference of the peak irradiance positions for different wavelengths $\delta_\lambda = Z_p(\lambda_1) - Z_p(\lambda_2)$, expressed along the optical axis [1]. In classical optics, an achromatic lens is designed to have the same focal length for two well-separated wavelengths, i.e. $\delta_\lambda = 0$.

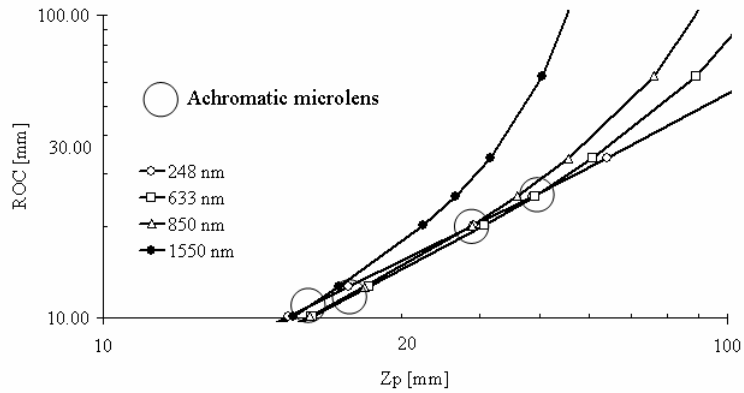

Fig. 8. ROC versus position of peak irradiance Z_p for a microlens of Ø = 635 µm, illuminated by a plane wave at four different wavelengths. The crossings between two curves corresponding to achromatic microlenses are shown with circles.

In Fig. 8, we observe that for each pair of wavelengths the different graphs are crossing in one point. From the UV to the IR a value for ROC is found where the longitudinal chromatic aberrations are zero for two different wavelengths. For our example of a microlens with diameter Ø = 635 µm, the peak radiance at 248 nm and 1550 nm are equal z_p(248 nm) = z_p(1550 nm) = 21.7mm for ROC = 10.8 mm, Fig. 7.

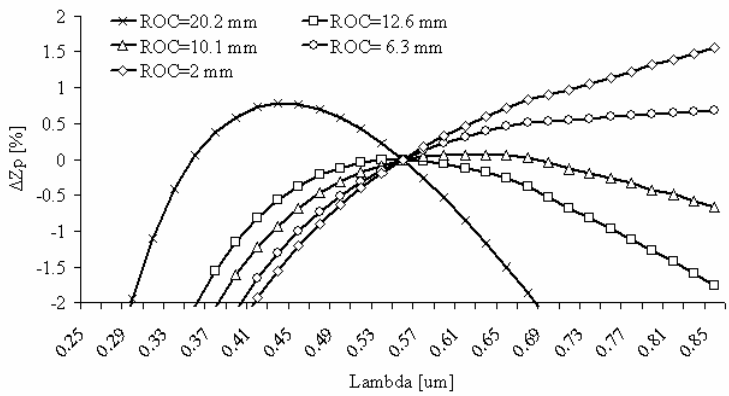

Fig. 9. Relative variations on Zp calibrated at 550 nm for five microlenses of Ø = 635 µm for five ROC, illuminated by a plane wave at different wavelengths.

Similar to classical achromats an achromatic microlens does not show an achromatic behavior over the full wavelength range in-between λ_1 and λ_2. The variation of achromats inside the range between these two design wavelengths is usually called secondary color aberration [1]. In classical optics the design of achromatic lenses can be made for any desired Z_p. In the present case, chromatic aberrations are directly related to the diameter and the ROC as these are the only free parameters. For a fixed diameter of microlenses, the appearance of diffraction effect, used for chromatic aberration corrections, depends on the ROC as seen in Fig. 6. This implies for each design one position of the peak irradiance.

To investigate an achromatic design for a microlens we fix a diameter. Then to allow comparisons a wavelength of reference fixing Z_p is required. It is now possible to plot the relative variations of this Z_p against the wavelength of a defined spectrum. For example, Fig. 9 shows the variations as function of the wavelength of Z_p expressed in percent of the Z_p calibrated at 550 nm. This is done for different ROC while for each lens Z_p at 550 nm is taken to normalize. The effect of diffraction appears when ROC increases. Correction of chromatic aberrations is possible for curve shapes that show a maximum in the desired wavelengths region. It would seem that small curvature (large radius of curvature) of the plot at the maximum would lead to small chromatic aberration in Fig. 9. Curves for ROC = 20.2 mm (FN = 4), 12.6 mm (FN = 6) and 10.1 mm (FN = 8) in Fig. 9 show a maximum. Note, that the FN are calculated at 550 nm. The maximum shifts to shorter wavelengths for increasing ROC. The microlens with a ROC fixed to 10.1 mm shows less than 1 ‰ variation on Z_p from 530 nm to 690 nm. For comparison the microlens with ROC=2 mm is not influenced by diffraction effects and shows more than 8 ‰ variations on Z_p inside the same range. For this wavelengths range we see from Fig. 9 that the lens with ROC=10.1 mm represents an optimum design for a lens of 635 μm diameter. The position of the peak irradiance is 21.5 mm.

6. Conclusion

It is well known from geometric optics that increasing the focal length of any lens leads to increase its ROC. This is the case for lenses having large values of FN >>1. By comparison, microlenses by their small diameters impose small value for ROC and then short focal length. When designing a microlens with large ROC, diffraction at the lens aperture may severely dominate the optical properties of the microlens and limit the range of the effective focal length. The upper limit of the focal length is determined by the diffraction pattern of a pinhole with equal diameter. Moreover refraction and diffraction have opposing influence on the position of the peak irradiance when changing the wavelength of illumination. Diffraction at the lens stop can be used to correct chromatic aberration introduced from the dispersion of the lens material. For microlenses with low Fresnel numbers (FN<10), achromatic designs can be realized in one single material.